J Mater Sci (2007) 42:889–900
DOI 10.1007/s10853-006-0007-x

Analysis of dislocation mechanisms around indentations through slip step observations

K. A. Nibur · F. Akasheh · D. F. Bahr

Received: 26 August 2005 / Accepted: 15 March 2006 / Published online: 3 January 2007

Abstract Atomic force microscopy has been used to study slip step patterns, which form around indentations in FCC alloys. These patterns form in a consistent and repeatable manner. From these observations it has been determined that slip steps increase in height only in the outer region of the plastic zone leading to the cessation of their growth as the plastic zone expands outward. Electron backscatter diffraction techniques are used to map grain orientation and the effect of different surface orientations as well as different tip geometries on slip step behavior is explored. Changes in resolved shear stress on different slip planes can be observed qualitatively from changes in the slip step patterns as surface orientation and tip geometry are varied. Pile up is shown to form above the regions with the largest amounts of strain downward into the bulk. Changes in slip step patterns can be predicted based on changes in resolved shear stress. Discreet dislocation dynamics simulations have been performed to support these observations.

Introduction

Slips steps provide a relatively simple way to observe deformation in crystalline materials. Earlier examples using slip steps to study deformation mechanism include optical microscopy observations of steps in nickel compression specimens [1] while more recent measurements have utilized newer techniques such as atomic force microscopy [2]. Although slip steps on the surface do not directly indicate what specific deformation mechanisms are taking place beneath the surface, they do result from those specific mechanisms. Therefore, slip step analysis can provide significant insight into deformation mechanisms beneath the surface if the proper correlation between the two is developed.

Much of the knowledge currently available in the literature in regard to the mechanics of indentations is based on phenomenological studies. Material properties commonly reported using indentation testing, such as hardness, can be measured and used for comparative purposes, however specific mechanistic information, such as why a material is harder or softer, cannot be gathered from a traditional indentation test alone. Nor can traditional hardness tests determine exactly how a minor change in microstructure or composition will change the bulk mechanical behavior of a material. Analysis of slip steps around indentations should provide a useful insight into the development of the plastic zone and the dislocation mechanisms taking place during deformation.

It has been shown in a previous paper that atomic force microscopy (AFM) can be used in conjunction with electron backscatter diffraction (EBSD) to identify specific slip planes responsible for any particular slip step visible on a material's surface around an indentation [3]. It was also shown that for a specific grain orientation and tip geometry, the patterns are highly repeatable [3]. Similar techniques have been used to identify slip steps around STM tip indentations in gold [4], within the cavity left by spherical indentations in MnZn ferrite [5], and around Berkovich

K. A. Nibur · F. Akasheh · D. F. Bahr (✉)
Mechanical and Materials Engineering, Washington State University, PO Box 642920, Pullman, WA 99164-2920, USA
e-mail: bahr@mail.wsu.edu

indentations in MgO and LiF [6–8]. Other examples of utilizing scanning probe techniques to examine the deformed region around an indentation have tended to focus on either the crystallographic nature of the extent of pile up and out of plane deformation [9] or the relationships between indentation impression and out of plane deformation [10]. To broaden the applicability of these measurement techniques, it will be necessary to develop a mechanism for the evolution of the observed slip steps with predictive capabilities to address changing variables such as surface orientation, tip geometry and different bulk mechanical properties of materials.

Relating surface slip steps to changes in deformation mechanisms could allow indentation testing to be a very powerful empirical benchmark for validating dislocation dynamics (DD) and meso-scale modeling simulations. TEM is often used as a tool for experimental validation of atomistic simulations, but it is often too limited in sample volume to be very useful for examining the larger length scales which can be employed in DD and combined multiscale finite element analysis (FEA)—DD simulations. In this way, problems such as hydrogen embrittlement and the contribution of grain boundaries to deformations can be modeled using DD simulations and experimentally verified using indentation testing.

This paper will present a number of observations relating to the emergence of slip steps around indentations in grains of different surface orientation and from tips with different geometries. Approximations of the stresses acting around indentations are developed which predict these observations. In addition, comparisons of dislocation dynamics simulations are presented to support some of these developments.

Experimental

Most of the experiments in this paper were performed in 21-6-9 stainless steel. This is a nitrogen strengthened austenitic alloy with the composition shown in Table 1. A few of the experiments used a commercially pure nickel alloy, Ni200. Both alloys were prepared by annealing in air to produce microstructures with large grains in excess of 1 mm in diameter in both alloys. Several samples of each material were cut from these annealed specimens and mechanically polished to a 0.05 μm colloidal silica finish. Each sample was then scanned using EBSD to reveal a map of the surface orientations of many grains across much of the sample area. These grain maps were then used to select large grains with orientations near {001}, {011} and {111} for subsequent indentation experiments.

Two types of indentation experiments were carried out in these selected grains. Conventional microhardness testing was performed using a Leco microhardness tester with a standard Vickers tip as well as a conical tip. In addition, instrumented indentation testing was done using a Nanoinstruments Nanoindenter II with a 90° conical tip. The conical tip used in the microhardness indenter is nominally a 90° tip but has a blunt tip radius of approximately 23 μm whereas the tip used in the Nanoindenter has a tip radius of approximately 1 μm. These tips will be referred to in this paper as the blunt and sharp conical tip, respectively.

Indentations were imaged post facto using contact mode AFM in a Park Autoprobe CP scanning probe microscope to reveal the formation of slip steps around indentations. Most AFM images presented in the paper are either deflection images or derivative images of height information to accentuate small surface features.

Results

This section will present results from many observations of slip steps around indentations. A variety of grain orientations and tip geometries will be presented to examine the effect of such variable on the formation of slip steps. A note on terminology presented at this point will eliminate some confusion during subsequent discussions of crystallography. Parallel, equidistant planes which are members of the {111} family with the same directional intersection with the surface will be referred to as sets of {111} planes. In this fashion there are four different sets of {111} slip planes in the FCC structure that can be resolved using atomic force microscopy. This will be used to differentiate non-parallel, equivalent slip planes without the confusion of arbitrarily assigning specific indices to the planes.

Table 1 Composition of the 21-6-9 stainless steel used in this study

Element	Fe	Cr	Ni	Mn	N	Al	C	O	P	S	Si
Wt %	Balance	19.1	6.9	9.5	0.26	0.012	0.034	0.0005	0.023	0.0002	0.51

Growth of the plastic zone and slip step morphology

As an indenter tip is pressed into a specimen, a region of material is plastically deformed around the indentation impression. This region is thought to be roughly hemispherical in shape for larger indentations [11, 12] and it is in the region where this plastic zone leaves the free surface that the slip steps will form. Two types of observations indicate that the slip steps form and grow near the outer edge of the plastic zone and after the plastic zone boundary is sufficiently far away, the step will cease to grow. This leads to an effective saturation height for slip steps.

The first such observation is shown in Fig. 1, where (a) shows a deflection signal AFM image of a 100 g (980 mN) Vickers indentation in nickel. Slip steps can be observed immediately at the edge of the indentation impression, and extend to the boundary between the plastic zone and elastic region beyond the indentation. This sample was then briefly polished to remove the pile up material and regain a flat surface, but not so much as to remove the residual indentation impression. The Vickers tip was carefully realigned with the impression and loaded to 200 g (1960 mN). Figure 1b is a deflection signal AFM image of this same indentation after being reloaded. After the subsequent indentation all of the slip steps further from the indentation were reactivated, however near the edge of the indentation very few slip steps continued to grow. This implies that the steps observed nearest the edge of the indentation were most likely formed during earlier stages of indentation. They ultimately end up at the very edge of the indentation only after the tip continued to penetrate deeper into the sample. As the depth continued to increase, the edge of the indenter overlapped into the pile up material and ''consumed'' the prior slip steps.

A second type of experiment provides additional evidence that slip steps near the indentation cease to grow as the plastic zone continues to expand and quantifies the saturation height of the steps. The height and spacing was measured for slip steps immediately next to instrumented indentations to various maximum loads in stainless steel. Figure 2a, b shows two typical indentations made with a sharp 90° conical tip at 20 mN and 500 mN peak loads into a grain with a surface orientation of (13 11 18), as determined by EBSD, in 21-6-9 stainless steel. Figure 2c shows cross section plots taken from 2 μm AFM scans of a region just beyond the left edge of each indentation. The average step height and spacing measurement technique is described elsewhere [13]. For the 500 mN indentation, the average step height was 7.1 μm and

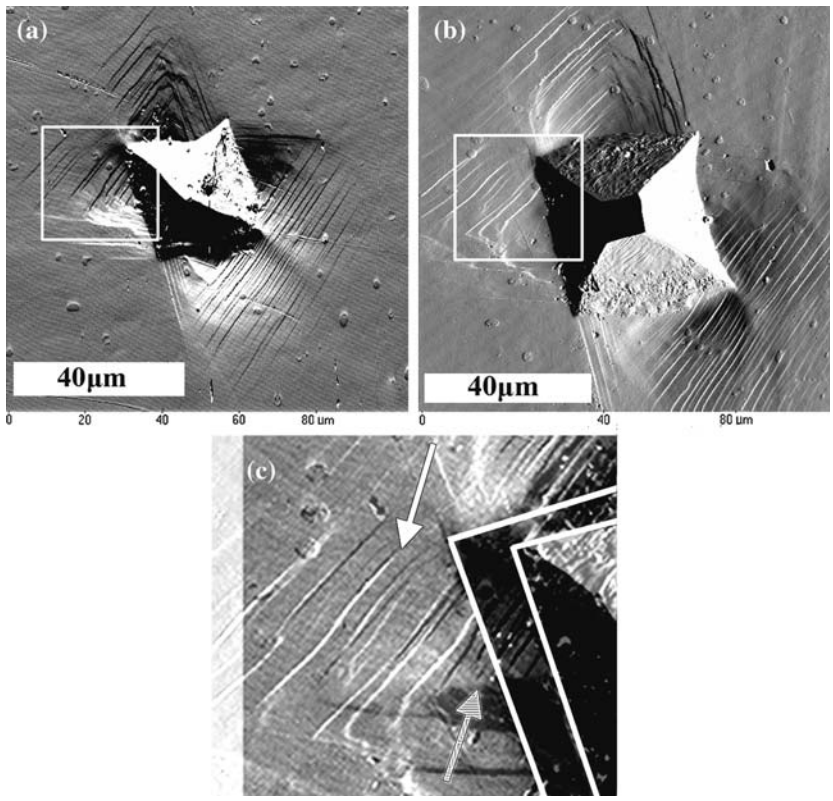

Fig. 1 A deflection signal AFM image of a 100 g (**a**) Vickers indentation shows slip steps immediately next to the indentation. The specimen was polished to remove the pile up material and slip steps only, then the indentation was enlarged at a load of 200 g (**b**). The region from within the boxes are overlaid in (**c**) where the white steps are from (b) and the black steps are from (**a**). Steps further away from the indentation line up indicating that the same steps continued to grow during the second loading as indicated by the white arrow. The hashed arrow points to steps near the indentation which formed during the first loading, but did not continue to grow during the second loading. The white lines outline the edges of both indentation impressions

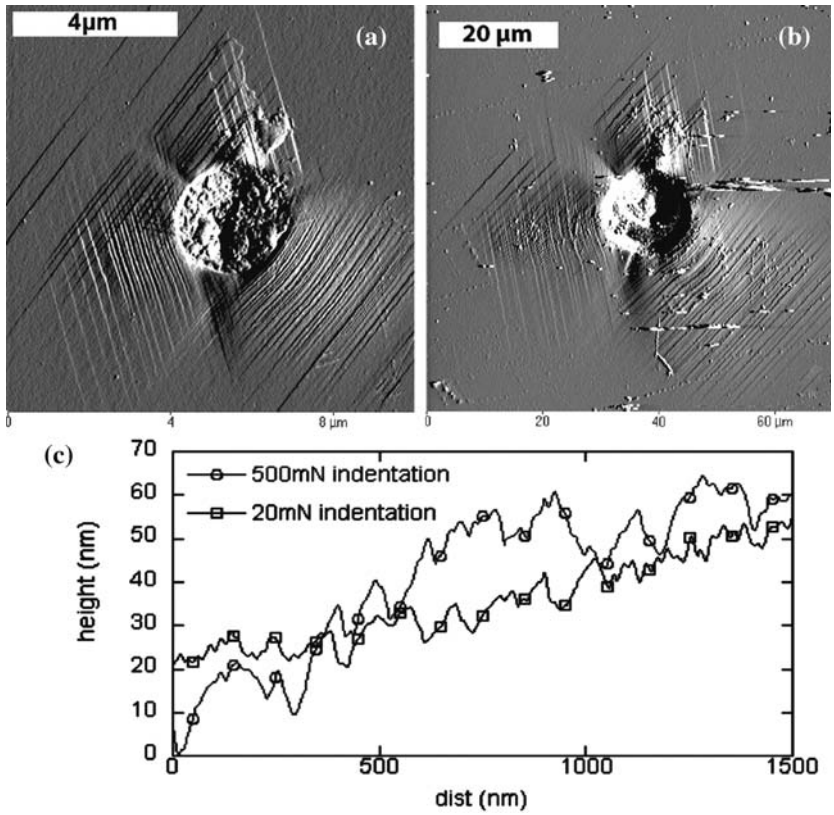

Fig. 2 Cross section plot (**c**) of slip steps very near the left side edge of a 20 mN (**a**) and 500 mN (**b**) indentation made into the same grain show that the height and spacing of the steps are very similar even for indentations of significantly different depths

the average spacing was 88 μm. The 20 mN indentation had an average step height of 5.6 μm and average spacing of 90 μm. A 250 mN indentation in this same grain had an average height of 4.8 μm with an average spacing of 86 μm. For indentations beyond 20 mN, the average step height and spacing is effectively constant near the indentation, and variations in step height are not related to changes in peak load.

Derivative AFM images also reveal differences in step morphology. Figure 3 is a schematic cross section representation of the slip steps around the indentation shown in Fig. 2a. The parallel slip steps to the lower right and upper left of the indentation all appear black in the derivative AFM image indicating that the steps on both sides of the indentation step up as the tip scans from left to right. The steps on the upper left side have a morphology that will be referred to as ''stair step'' type steps which are depicted by the left side of Fig. 3. This step morphology forms from slip planes for which the angle measured from the indentation load axis to the slip plane normal would be a positive value. These will be referred to as ''positively inclined'' slip planes. Similarly, the steps to the lower right of the indentation in Fig. 2a step up as the imaging tip moves away from the indentation and have a morphology represented by the right side of Fig. 3. These will be referred to as ''serrated'' steps and form from the ''negatively inclined'' slip planes.

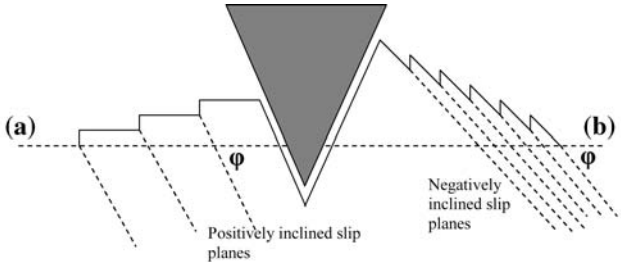

Fig. 3 Slip planes which extend into the material under the indenter tend to form slip steps with ''stair step'' morphology whereas slip steps that extend into the material away from the indenter tend to form a ''serrated'' morphology

Effect of surface orientation

Indentations were made into multiple grains with different surface orientations to observe the effects of crystal orientation on the slip step patterns formed. Patterns were observed in polycrystalline stainless steel and nickel for various grains, particularly with orientations near {001}, {011} and {111} as well as for a (111) single crystal of nickel. Figure 4 shows indentations made into five different surface orientations: (a) (1 2 30), (b) (0 1 8), (c) (8 5 2), (d) nickel (111), (e) (13 11 18). Slip

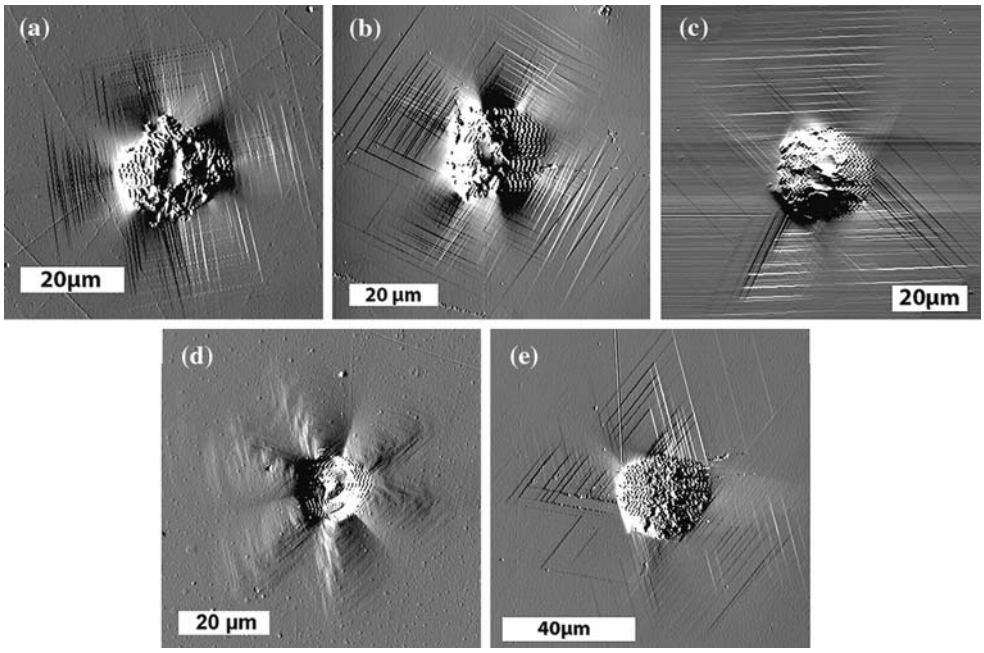

Fig. 4 Indentations made into surfaces of various orientations: (**a**) (1 2 30); (**b**) (0 1 8); (**c**) (8 5 2); (**d**) nickel (111); (**e**) (13 11 18)

step patterns in the (1 2 30) orientation behave similar to that which would be expected from a perfect (001). Four distinct regions of pile up occur and each contain slip steps from a different set of {111} slip planes. Within each of these pile-up regions, slip on other sets of {111} planes does not reach the free surface and produce slip steps. All of the slip steps result from the positively inclined set of slip planes. When the surface rotates a bit further away from (001), such as with the (0 1 8) orientation, there still remain four distinct pile up lobes. However, two of them (those to the upper and lower left sides in Fig. 4b) contain slip steps from only the positively inclined slip planes, while the other two lobes of pile up contain slip steps from both the positively and negatively inclined sets of slip planes.

The (8 5 2) orientation behaves somewhat similarly to a (110) surface. The indentation shown in Fig. 4c has a slip step pattern consisting of long, parallel slip steps shown in the figure both above and below the residual indentation impression. These steps all belong to the same set of {111} slip planes such that they are positively inclined on one side of the indentation and negatively inclined on the other, as illustrated in Fig. 3. The discontinuity of these steps near their middle is therefore not a result of dislocations moving on different sets of planes, but rather an indication that they do not all have the same Burgers vector. Repulsion from opposite components of the Burgers vectors would limit the expansion of dislocation loops.

Figure 4d is an indentation made into a (111) single crystal of nickel. This pattern shows parallel slip steps from each of the three other sets of {111} slip planes that are not parallel to the surface. The slip steps, and resulting pile up, is very symmetrical around the indentation. Figure 4e shows an indentation into 21-6-9 stainless steel with a surface orientation of (13 11 18). The slip steps to the upper and left side of the indentation form in a pattern consistent with that seen by the perfect (111) surface seen in Fig. 4d, however they do not form symmetrically around the indentation. Topographic images confirm that the pile up is mostly confined to those regions were the slip steps are seen and very little pile up occurs on the other side of the indentation.

Effect of tip geometry/orientation

There are distinct differences between the slip step patterns which result from the sharp and blunt conical tips. Figure 5a, b shows the result of indentations made with the (a) sharp and (b) blunt tips into a (0 1 8) oriented surface. The sharper tip produces more pile up and the resulting slip steps are spaced much closer together.

Figure 5c, d shows Vickers indentations in this same (0 1 8) grain. In Fig. 5d the tip was rotated 45° about the loading axis with respect to that shown in Fig. 5c. Figure 5c shows a ''sharp'' orientation for the tip where the faces of the pyramid are aligned parallel with the {111} slip planes. This results in slip step patterns which appear similar to those which result from the sharp conical tip. Likewise, the Vickers tip exhibits a ''blunt''

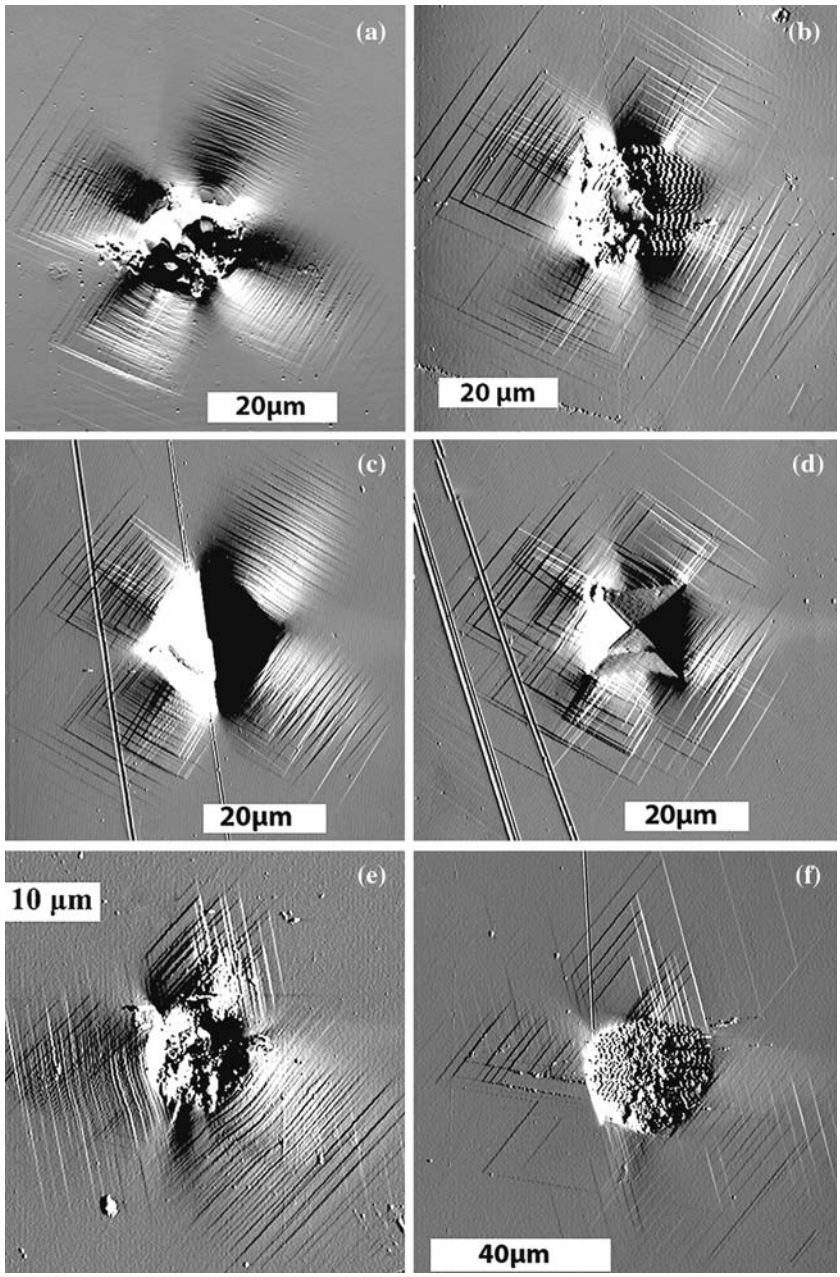

Fig. 5 Slip steps patterns which result from (**a**) sharp tip and (**b**) blunt tip in (0 1 8) surface orientation, as well as Vickers indentations oriented at 45° rotations (**c**), (**d**), and sharp tip (**e**) and blunt tip (**f**) indentation into a surface with (13 11 18) orientation

orientation, shown in Fig. 5d, which results when the projection of the faces of the tip are not aligned parallel with the {111} planes of the sample. This orientation produces slip step patterns which appear similar to those produced by the blunt conical tip.

Figure 5e shows a sharp tip indentation into a grain with a surface orientation of (13 11 18) and (f) shows an indentation made in this same grain with the blunt tip. The blunt tip produced only a small amount of pile up, which occurs on the positively inclined slip planes and its bounding planes. The sharp tip results in only a small amount of additional growth of those steps, but adds a significant increase to the total amount of pile up via closely spaced steps on the negatively inclined planes to the left of and below the indentation as shown in Fig. 5e.

Discussion

Contribution of elastic stresses

At the initial onset of plasticity in any indentation process the only strains present are due to the elastic stresses. These strains are primarily directed away from the indentation and into the bulk of the material and,

therefore, do not contribute to out-of-plane deformation, or pile up around the resulting indentation. Out of plane deformation occurs only after the plastic strain has reached a value at which the elastic expansion of the surrounding material can no longer accommodate the displaced volume of the indentation [11].

The elastic stresses present during the early stages of indentation can be estimated as the elastic stresses due to a concentrated normal force applied to an elastically isotropic solid. Using cylindrical coordinates with the axis of indentation in the z direction these stresses are [11]:

$$\sigma_r = \frac{P}{2\pi}\left\{(1-2v)\left(\frac{1}{r^2}-\frac{z}{\rho r^2}\right)-\frac{3zr^2}{\rho^5}\right\} \quad (1)$$

$$\sigma_\theta = \frac{P}{2\pi}(1-2v)\left(\frac{1}{r^2}-\frac{z}{\rho r^2}-\frac{z}{\rho^3}\right) \quad (2)$$

$$\sigma_z = -\frac{3P}{2\pi}\frac{z^3}{\rho^5} \quad (3)$$

$$\tau_{rz} = -\frac{3P}{2\pi}\frac{rz^2}{\rho^5} \quad (4)$$

where P is the concentrated point force, r and z are the positions in the radial and axial directions, respectively, v is Poisson's ratio, and

$$\rho = \sqrt{r^2+z^2} \quad (5)$$

These stresses can be resolved on slip planes using Schmid's law as shown in Fig. 6. Parallel slip planes on either side of the indentation and inclined at an angle φ to the surface will be subjected to a radially symmetric stress state such that the normal stresses will be equal, but the shear stress component will have opposite sign. The resolved shear stress will therefore not be equal at different points around the indentation. Figure 7 shows the resolved shear stress evaluated at a position, such that $r = z$, as a function of the angle (φ) between a slip plane and the surface plane for slip planes with any angle between 0° and 90°. Positively and negatively inclined slip planes are plotted as lower and upper curves respectively. A slip plane at an inclination of 45° will have no resolved component due to τ_{rz} and so the total resolved stress resulting from σ_r and σ_z will be the same on both planes. For angles greater than 45° the slip plane with negative inclination will have the higher

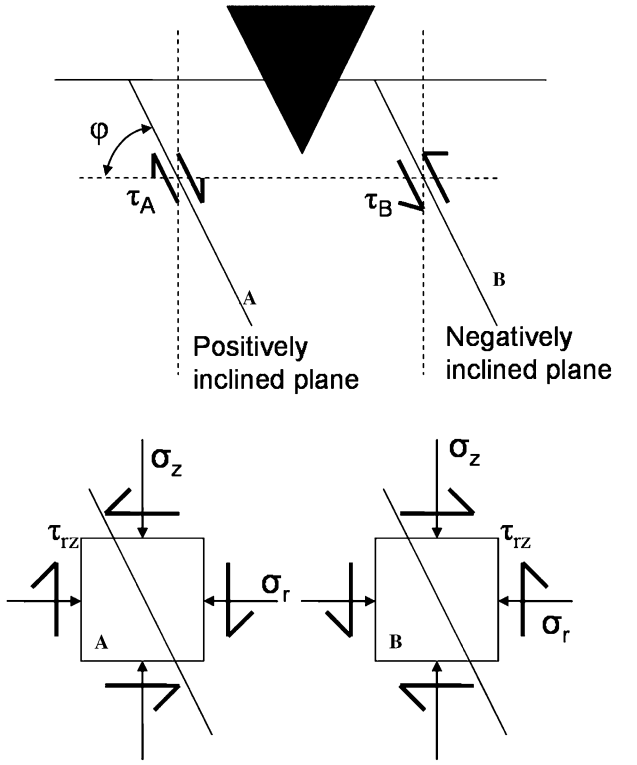

Fig. 6 The elastic stresses from a point loading will produce an axisymetric stress field such that parallel slip planes on either side of an indentation will experience the same normal stresses, but the shear component will have the opposite sign. The result of this is that when the plane is inclined at an angle greater than 45° with respect to the surface, the negatively inclined slip plane will have a larger resolved shear stress, while the positively inclined plane will have a larger resolved stress in the inclination is less that 45°

resolved shear stress, and for angles less than 45° the slip plane with positive inclination will have the greater resolved shear stress.

When little or no pile up occurs around an indentation these calculations for the elastic stresses around an indentation can be appropriate for predicting where slip steps will occur. The slip steps within spherical indentations [5] and the slip lines which extend along the surface away from Berkovich indentations in MgO [6] both accommodate downward material flow. These slip steps are very different than those shown in the observations in this paper, which accommodate the upward flow of material pile up. Other studies have observed rosette patterns of either slip steps or dislocation etch pits around indentations [7, 14, 15]. It is important to note that most of the materials examined in these studies do not exhibit significant pile up around the indentations. Therefore, their formation occurs due to a different phenomenon than that which causes the slip steps in regions of material pile up.

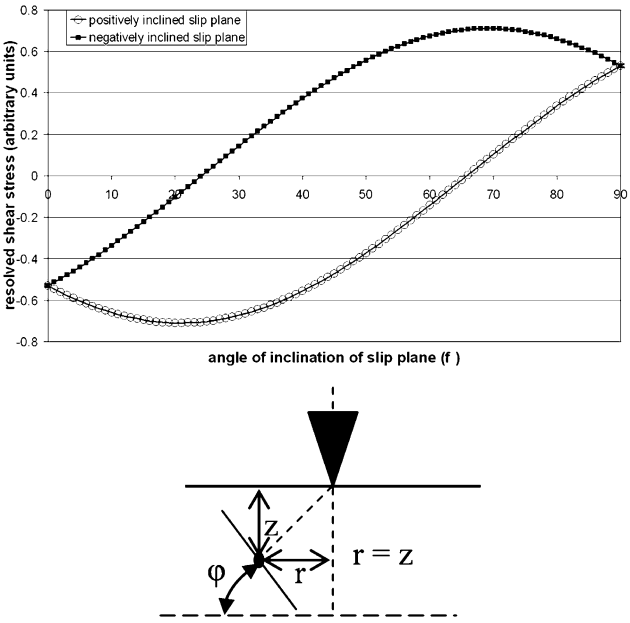

Fig. 7 The resolved shear stress acting on a slip plane is plotted in arbitrary units for planes inclined at an angle φ with respect to the surface. The plot is evaluated for any point where $r = z$ and the actual magnitude of the resolved stress will decrease with the distance from the point of loading and increase with applied load. The top curve represents the stress on a positively inclined plane whereas the lower is the stress on a negatively inclined slip plane

Indentations with pile up

The observations in this paper clearly indicate that the slip steps visible on the surface around indentations in materials that pile up are either the result of, or result from, the pile up. If pile up occurs as a result of the sub-surface strain exceeding that which elastic expansion can accommodate, then downward flow should precede the pile up. This implies the necessity to look for signs of sub-surface downward flow even when pile up is clearly present. This has been observed most clearly from the blunt tip indentation into a (13 11 18) surface shown in Fig. 4e. The surface slip steps, seen in the derivative AFM image in (e) show that pile up is largely limited to two distinct lobes on the left and above the indentation. For this particular surface orientation, which is rotated about 12° from a perfect (111) surface, there are three slip planes that are oriented favorably for slip down into the bulk and the other, the (111), is nearly parallel to the surface. Of the other three slip planes, the $(11\bar{1})$ is inclined 82° to the surface, the $(\bar{1}11)$ is 68° and the $(1\bar{1}1)$ is at 62°. Figure 8, the resolved shear stress as a function of the angle of inclination of a slip plane to the surface, is similar to Fig. 7, except that the resolved stress is evaluated where $r = z/10$, which corresponds to 5.7° from the indentation axis, nearly directly beneath the indentation. It can be seen from Fig. 8 that for all three of these slip planes, the resolved shear stress will be higher on the negatively inclined slip plane. In addition, the resolved shear stress on the $(1\bar{1}1)$, at 62°, is the highest, at 68°, the $(\bar{1}11)$ is slight lower, and the lowest is on the $(11\bar{1})$ at 82°. Downward flow of material should occur on the $(1\bar{1}1)$ and $(\bar{1}11)$ slip planes prior to occurring on the $(11\bar{1})$.

To examine the correlation with computational simulations of dislocation dynamics, corresponding simulations were performed using methods described in detail elsewhere [16]. These simulations predicted increased dislocation activity on the $(1\bar{1}1)$ and $(\bar{1}11)$ planes than on the $(11\bar{1})$ as shown in Fig. 9a, b. For this simulation, the surface was rotated 10° about the $(01\bar{1})$ direction which results in a surface normal of approximately (13 13 18), very similar to the (13 11 18) surface which is shown indented in Fig. 9c. The overlay of the three slip planes demonstrates the direction of downward material flow due to each of the planes. The two regions of greater pile up correspond with the regions of greater sub-surface strain due to the more active $(1\bar{1}1)$ and $(\bar{1}11)$ planes.

In this manner greater upward flow, i.e. larger pile up, would occur above the regions with the greatest downward strains. The claim has often been made that pile up occurs where the stress field aligns with the crystallographically preferred slip systems [17]. While this general statement cannot be argued, this current study suggests it might be more accurate to note that pile up will occur above the regions with significant

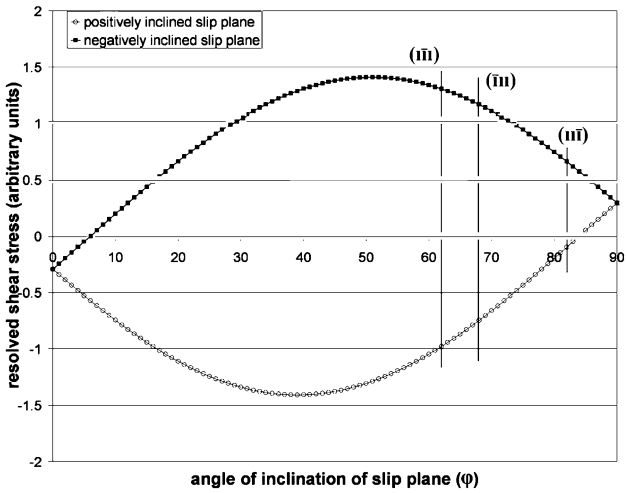

Fig. 8 The resolved shear stress measured 5.7° from the axis of indentation changes with the angle of inclination of the slip plane, which is measured with respect to the surface plane

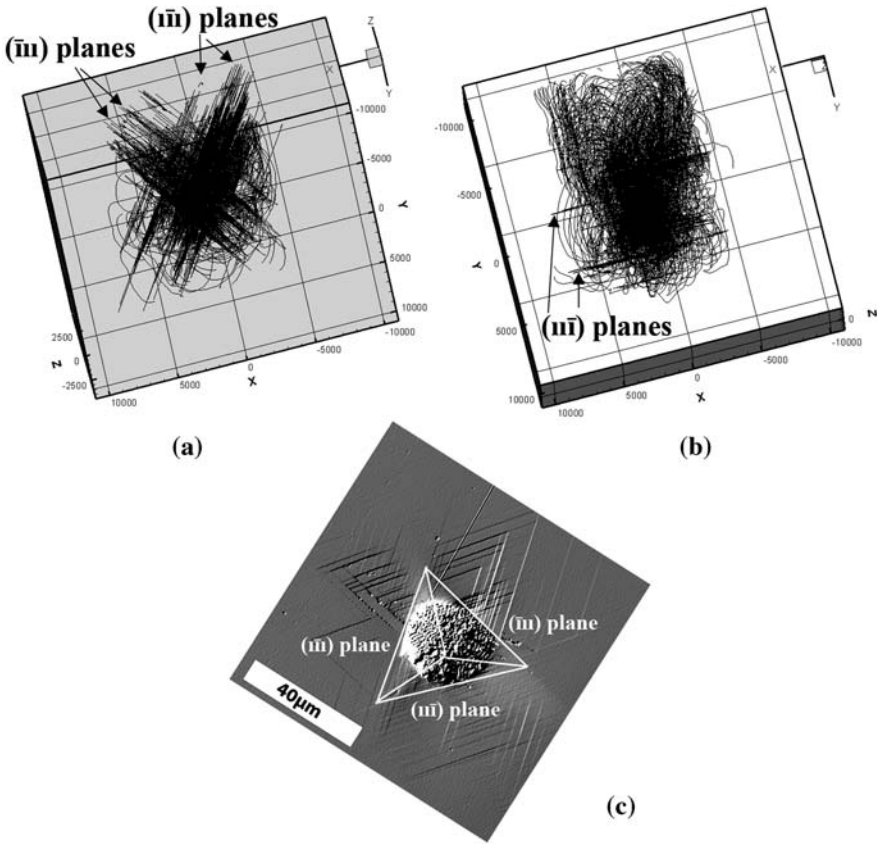

Fig. 9 Dislocation dynamics simulations show a high concentration of dislocation loops on the ($\bar{1}$11) and (1$\bar{1}$1) slip planes (**a**) and only limited activity on the (11$\bar{1}$) planes for a surface rotated 10° for (111). This orientation is very similar to the (13 11 18) surface shown indented in (**c**). The planes with higher dislocation activity correspond to the regions of greater pile up around the indentation

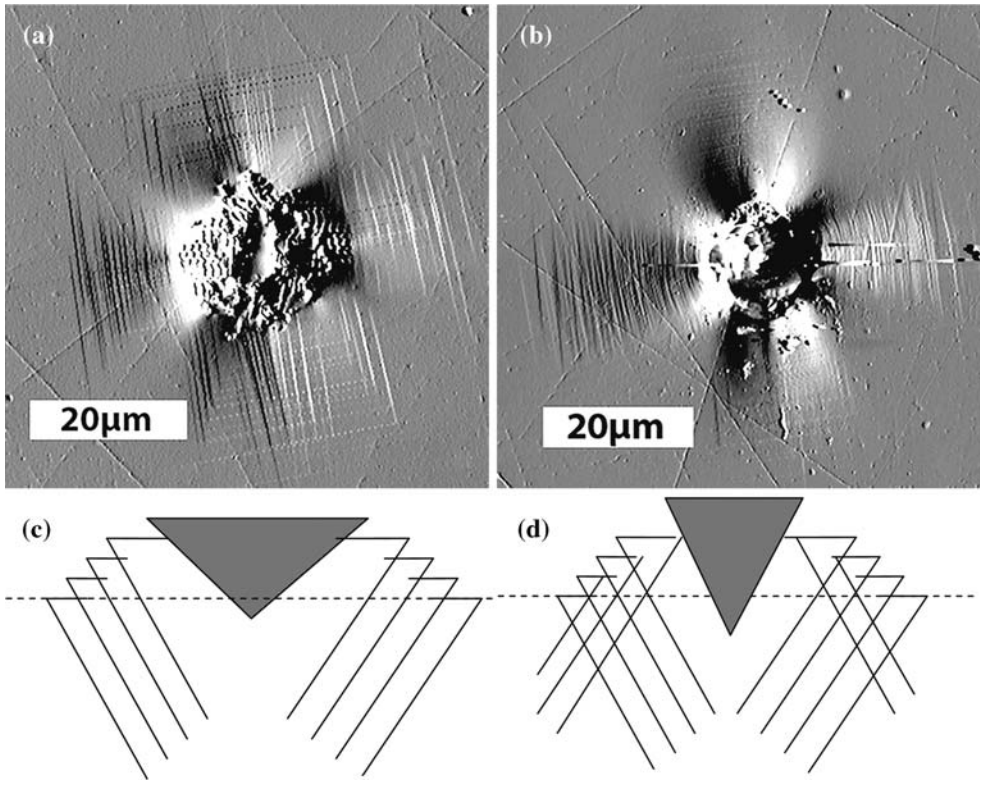

Fig. 10 Slip steps form only from the positively inclined slip planes around blunt tip indentations in a grain with surface orientation of (1 2 30). When the effective strain is increased by using a sharp tip, steps form from both the positively and negatively inclined slip planes

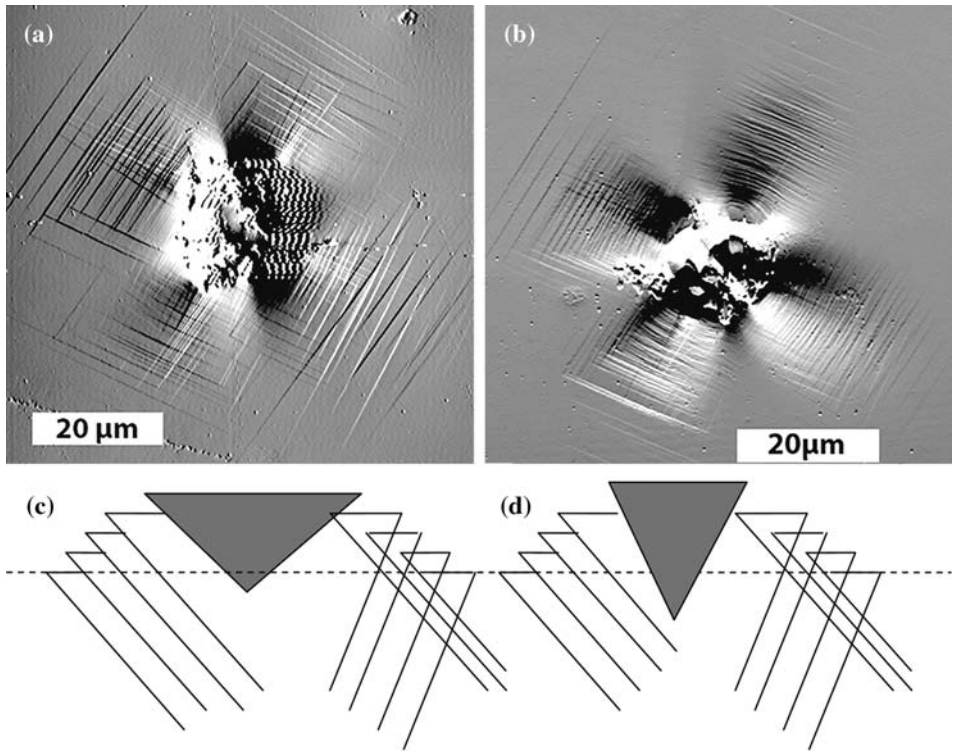

Fig. 11 When indentations are made into a grain with surface orientation of (0 1 8), slip steps form from only the positively incline slip plane on one side, but from both the positively and negatively inclined slip planes on the other side. Increasing the strain by using a sharp tip increases the number of slip steps and pile up height but does not appear to change this distribution significantly

downward flow of material. This downward flow will be dependant on the alignment of the indentation stress field with the slip systems capable of supporting that flow. Therefore, it should be possible to predict pile up behavior based primarily on the slip systems oriented for downward flow.

Assessment of stresses during pile up

Once pile up is occurring, the elastic back stress of the bulk is responsible for pushing material to the surface, suggesting that it will be valuable to explore some of the necessary mechanisms for this. When a blunt tip indentation is made into a (1 2 30) oriented surface of 21-6-9, slip steps form with the symmetry expected for a perfect (001) crystal as shown in Fig. 10a. All of the slip steps occur from the positively inclined slip planes, as is represented by the schematic cross section shown in Fig. 10c. Figure 10b, d demonstrates that as the strain is increased by indenting with a sharper tip, slip steps begin to form from the negatively inclined slip planes. This would indicate that the resolved shear stress is greater on the positively inclined slip plane, but as the strain is increased by using a sharper tip, the resolved shear stress on the negatively inclined slip plane will reach a value large enough to cause slip.

If this is the case, then rotating further from (001) should cause the distribution of resolved stresses on the positive and negatively inclined planes to differ for one side of the indentation with respect to the other. This was tested by performing indentations in a grain with surface orientation of (018) as shown in Fig. 11. Indentations made with a blunt tip into this grain show slip steps from only the positively inclined slip planes on one side, but from both planes on the other side. On the left side (as depicted in Fig. 11), φ, the angle of inclination of the slip plane with respect to the surface, decreased from its value in a perfect (001) surface for

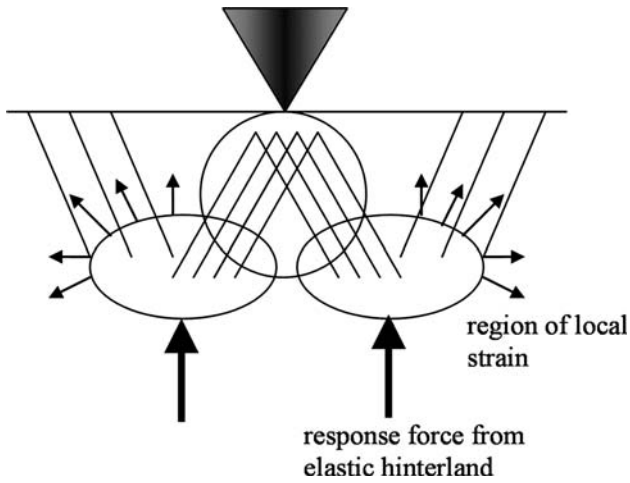

Fig. 12 This schematic demonstrates a possible mechanism by which downward strains below the indentation could lead to regions of higher stress beneath the surface which in turn act to promote slip back to the surface to produce out-of-plane pile up

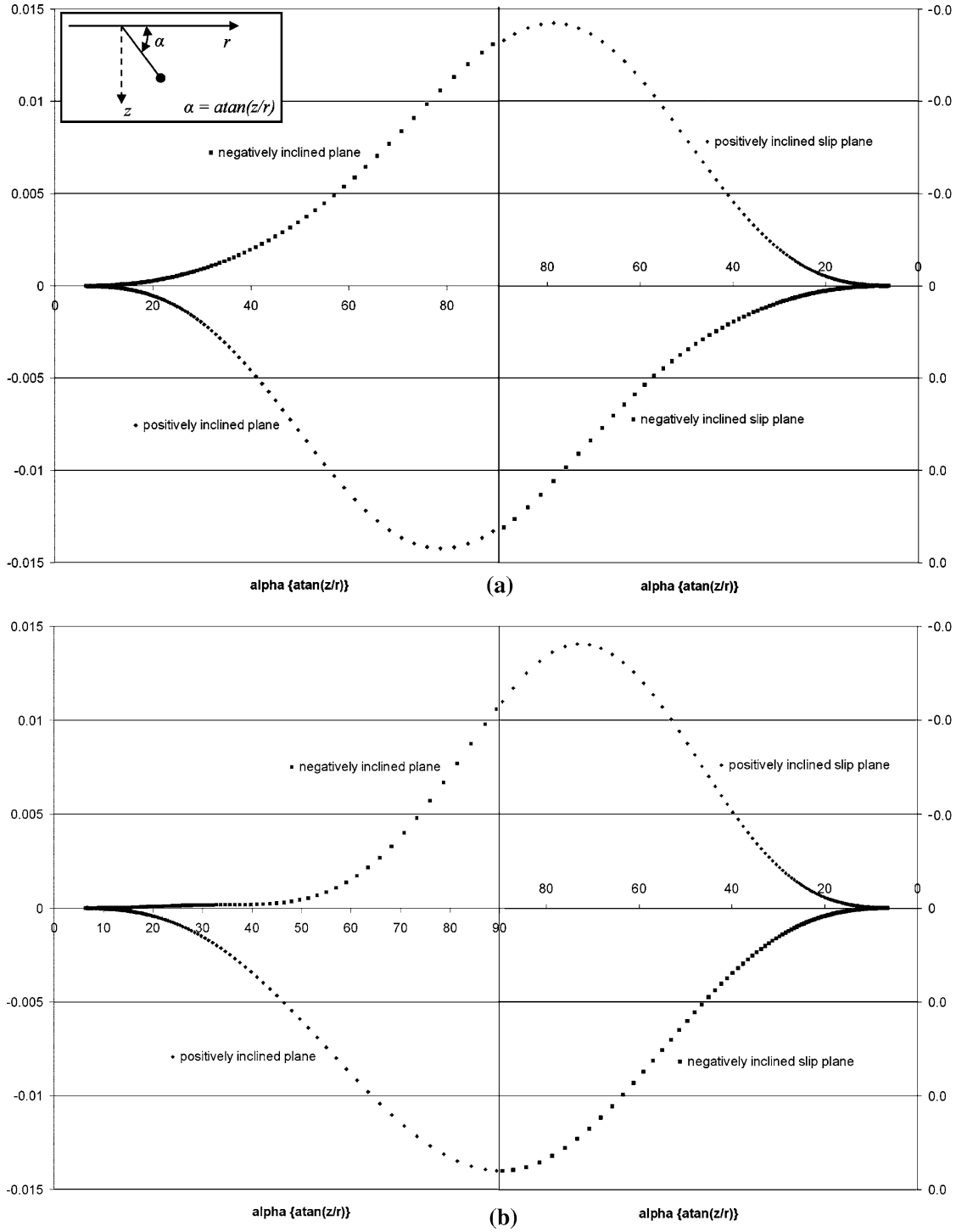

Fig. 13 Resolved shear stress resulting from the loading elastic response is plotted as a function of angular position $\alpha = \text{atan}(z/r)$. The maximum resolved shear stress is always on the positively inclined slip plane for the perfect (001) orientation (**a**). When the surface rotated 10° from (001) (**b**) the resolved stress on the negatively inclined slip plane is significantly lower than that on the positively inclined slip plane on the left side of the indentation. On the right side, both planes experience similar resolved stresses

the positively inclined slip plane, and increased for the negatively inclined slip planes. This results in an increased difference in the resolved shear stress between the sets of slip planes. On the right side, the opposite occurs, resulting in a decrease in the difference between the resolved shear stress for each family

of planes. When the strain is increased by using a sharper tip, the steps on the left side still form only from the positively inclined slip plane. On the right side, steps form from both slip planes, with the negatively inclined plane becoming the dominant source of the steps.

The assumption that pile up results from the response of the elastic stresses in the surrounding material implies that the actual stress state which produces the pile up is not solely based on the stress field of the indenter tip itself. A first order estimate of the response of the elastically strained surrounding material can be made by assuming a point loading exists beneath each region of localized strain. Figure 12 demonstrates this situation schematically. Downward flow on slip systems predicted by the elastic stresses produced from the indenter tip produced regions of localized strain beneath the surface. This strain induces an elastic response which pushes material back toward the free surface.

The resolved shear stress which would result from the elastic response when modeled as a point load at the elastic–plastic boundary is shown in Fig. 13. In part (a) a perfect (001) surface is assumed and the resolved shear stress is plotted as a function of angular position, α, in the r,z plane beneath the indentation where $\alpha = \text{atan}(z/r) = 90^{\circ}$ is directly above the point load. Figure 13b quantifies the resolved shear stress when the surface is rotated 10°. It can be seen that on the left side of the indentation the positively inclined slip plane will still have the larger magnitude resolved shear stress, whereas on the right side the negatively inclined slip plane will now have the larger resolved shear stress. However, the similarity in magnitude between the positive and negative inclinations suggests that it would be likely both slip systems would be active, particularly given the approximations inherent in this model. This corresponds to the experimental results shown in Fig. 11 for indentations in a surface with (018) orientation, where both the positive and negative inclination slip planes produce surface steps on the right side of the indentation.

Conclusions

Slip steps in engineering alloys appear around indentations in a consistent and repeatable manner and provide a means to extract dislocation behavior from quasistatic indentation testing. The steps form in the outer region of the plastic zone, and as the plastic zone continues to expand outward, individual steps saturate and will cease to grow larger. The general form of the patterns created by the slip steps is dependant on crystal orientation while tip geometry has less significant effects. Vickers indentations can produce both ''sharp'' and ''blunt'' slip step behavior based upon the orientation of the tip diagonals with respect to the crystallographic orientation. The elastic stresses generated from a concentrated point loading have been used to estimate the stresses responsible from downward flow of material around an indentation, and a simple model describing the effects of sample orientation has been experimentally verified. Indentations that probe volumes on the order of cubic micrometers produce well developed plastic zones with dislocation structures comparable to those around larger indentation tests.

Acknowledgements Funding was provided by the United States Department of Energy and Sandia National Laboratories through the Presidential Early Career Award for Scientists and Engineers program under contract DE-AC04-94AL85000. The authors wish to thank Prof. H.M. Zbib of Washington State University for assistance with the dislocation dynamics simulations and Dr. B.P. Somerday of Sandia National Laboratories for helpful discussions.

References

1. McInteer WA, Thompson AW, Bernstein IM (1980) Acta Metall 28:887
2. Gerberich WW, Harvey SE, Kramer DE, Hoehn JW (1998) Acta Mater 46:5007
3. Nibur KA, Bahr DF (2003) Scripta Mater 49:1055
4. Carrasco E, Gonzalez MA, Rodriguez de la Fuente O, Rojo JM (2004) Surf Sci 572:467
5. Kadjik SE, Broese Van Groenou A (1989) Acta Metall 37:2625
6. Tromas C, Girard JC, Audrier V, Woirgard J (1999) J Mater Sci 34:5337
7. Gaillard Y, Tromas C, Woirgard J (2003) Phil Mag Lett 83:553
8. Gaillard Y, Tromas C, Woirgard J (2003) Acta Mater 51:1059
9. Stelmashenko NA, Walls MG, Brown LM, Milman YUV (1993) Acta Metall Mater 41:2855
10. Woodcock CL, Bahr DF (2000) Scripta Mater 43:783
11. Johnson KL (1985) Contact mechanics, Cambridge University Press, 50, pp 171–176
12. Samuels LE, Mulhearn TO (1957) J Mech Phys Sol 5:125
13. Nibur KA (2005) PhD Thesis. Washington State University
14. Zielinski W, Huang H, Gerberich WW (1993) J Mater Res 8:1300
15. Hu SM (1975) J Appl Phys 46:1470
16. Zbib HM, Diaz de la Rubia T (2002) Int J Plasticity 18:1133
17. Stelmashenko NA, Walls MG, Brown LM, Milman YuV (1993) Acta Metall Mater 41:2855